Biogeosciences Open Access
Discussions

Coral records of reef-water pH across the central Great Barrier Reef, Australia: assessing the influence of river runoff on inshore reefs

J. P. D'Olivo[1,2,3], M. T. McCulloch[1,2], S. M. Eggins[3], and J. Trotter[2]

[1]The ARC Centre for Excellence for Coral Reef Studies, Australia
[2]School of Earth and Environment, The University of Western Australia, Crawley 6009, Australia
[3]Research School of Earth Sciences, Australian National University, Canberra 0200, Australia

Correspondence to: J. P. D'Olivo (juan.dolivocordero@uwa.edu.au)

Discussion Paper | Discussion Paper | Discussion Paper | Discussion Paper |

BGD

11, 11443–11479, 2014

Coral records of reef-water pH across the central Great Barrier Reef, Australia

J. P. D'Olivo et al.

Title Page

Abstract | Introduction

Conclusions | References

Tables | Figures

|◀ | ▶|

◀ | ▶

Back | Close

Full Screen / Esc

Printer-friendly Version

Interactive Discussion

Full Screen / Esc

Printer-friendly Version

Interactive Discussion

Abstract

The boron isotopic ($\delta^{11}B_{carb}$) compositions of long-lived *Porites* coral are used to reconstruct reef-water pH across the central Great Barrier Reef (GBR) and assess the impact of river runoff on inshore reefs. For the period from 1940 to 2009, corals from both inner as well as mid-shelf sites exhibit the same overall decrease in $\delta^{11}B_{carb}$ of 0.086 ± 0.033‰ per decade, equivalent to a decline in seawater pH (pH_{sw}) of $\sim 0.017 \pm 0.007$ pH units per decade. This decline is consistent with the long-term effects of ocean acidification based on estimates of CO_2 uptake by surface waters due to rising atmospheric levels. We also find that compared to the mid-shelf corals, the $\delta^{11}B_{carb}$ compositions for inner shelf corals subject to river discharge events, have higher and more variable values and hence higher inferred pH_{sw} values. These higher $\delta^{11}B_{carb}$ values for inner-shelf corals are particularly evident during wet years, despite river waters having lower pH. The main effect of river discharge on reef-water carbonate chemistry thus appears to be from higher nutrients driving increased phytoplankton productivity, resulting in the drawdown of pCO_2 and increase in pH_{sw}. Increased primary production therefore has the potential to counter the more transient effects of low pH river water (pH_{rw}) discharged into near-shore environments. Importantly however, inshore reefs also show a consistent pattern of sharply declining coral growth that coincides with periods of high river discharge. This occurs despite these reefs having higher pH_{sw} values and hence higher seawater aragonite saturation states, demonstrating the over-riding importance of local reef-water quality on coral reef health.

1 Introduction

Coral reefs are under threat, not only from the global effects of CO_2 driven climate change but also direct local impacts from, for example, disturbed river catchments and hence degraded water quality (McCulloch et al., 2003). Changing land-use practices since the arrival of European settlers has produced increased discharge of terrestrial

material from the Burdekin River into the Great Barrier Reef (GBR; McCulloch et al., 2003; Lewis et al., 2007). This has resulted in a decrease in water quality mainly in the form of increased nutrients and decreased water clarity (Brodie et al., 2010a; Fabricius et al., 2014), these effects being stronger closer to the coast. Known impacts

5 include the promotion of intense and extensive phytoplankton blooms and the increase in abundance of macro-algae (Devlin and Brodie, 2005; Brodie et al., 2010a). Changes in water quality within inner-shelf environments of the GBR have also been linked to a decrease in coral calcification (D'Olivo et al., 2013), coral biodiversity (De'ath and Fabricius, 2010), decreased coral cover (Sweatman et al., 2011), and crown-of-thorns

10 starfish outbreaks (Brodie et al., 2005).

Despite these studies, the effect of river flood plumes on the carbonate status of reef-waters, a fundamental property controlling calcification, remains largely unknown. It is commonly assumed that since both the salinity and pH of plume waters (pH_{pw}) are generally much lower than ocean waters, a decrease in aragonite saturation state

15 (Ω_{arag}) might be anticipated (Salisbury et al., 2008), with consequent negative affects for coastal calcifying organisms such as corals (e.g. Kleypas, 1999; Doney et al., 2009; McCulloch et al., 2012). The effect of lower seawater pH (pH_{sw}) could however be offset by the input of nutrients associated with river plumes, as in semi-isolated environments (e.g. enclosed lagoons) and/or highly productive areas where biological processes ac-

20 tively modify the local seawater chemistry (e.g. Hinga, 2002; Andersson et al., 2005; Bates al., 2010; Drupp et al., 2011; Falter et al., 2013; Duarte et al., 2013). For example, increased productivity during phytoplankton blooms can cause pH_{sw} to rise significantly (Hinga, 2002). Nutrient enhanced photosynthetic activity has been shown to amplify the seasonal pH cycle by more than 0.5 pH units in experiments within marine

25 enclosures in Narragansett Bay, Rhode Island (Frithsen et al., 1985), and to increase pH_{sw} by 0.7 units in the Peruvian coastal upwelling zone (Simpson and Zirino, 1980). In the GBR, it is not known to what extent terrestrial runoff and the associated phytoplankton blooms influence pH_{sw} and hence coral calcification, which is partly due to the lack of longer-term pH_{sw} measurements.

The δ^{11}B composition of biogenic carbonates (δ^{11}B$_{carb}$) is an established paleo-proxy for pH$_{sw}$, first developed by (Vengosh et al., 1991) and (Hemming and Hanson, 1992) and more recently refined for coral based studies by Trotter et al. (2011). The method relies on the preferential incorporation of the isotopically lighter B(OH)$_4^-$ over the B(OH)$_3$ species into marine carbonate skeletons, with the relative boron species concentration and isotopic compositions being pH dependent (Vengosh et al., 1991; Hemming and Hanson, 1992; Hönisch et al., 2004). Its application to corals has been validated (Hönisch et al., 2004; Reynaud et al., 2004; Trotter et al., 2011) and used for long-term pH$_{sw}$ reconstructions using massive *Porites* corals (Pelejero et al., 2005; Liu et al., 2009; Wei et al., 2009; Shinjo et al., 2013). Although coral δ^{11}B$_{carb}$ compositions closely parallel variations in pH$_{sw}$ (Hönisch et al., 2004; Krief et al., 2010; Trotter et al., 2011; McCulloch et al., 2012) there is a consistent species-specific positive offset of coral δ^{11}B$_{carb}$ compositions above the borate δ^{11}B value for ambient pH$_{sw}$ (Trotter et al., 2011; McCulloch et al., 2012). This elevation of pH was recently shown to be consistent with the physiological up-regulation of pH at the site of calcification to promote aragonite precipitation (Trotter et al., 2011; McCulloch et al., 2012). Trotter et al. (2011) quantified this internal pH offset and consequently derived ambient seawater values based on the systematic relationships they observed between the measured coral δ^{11}B$_{carb}$ composition and pH$_{sw}$.

In this study we present annual coral δ^{11}B$_{carb}$ data from cores of five massive *Porites* heads collected from two inner-shelf reefs and two mid-shelf reefs of the central GBR (Fig. 1). The δ^{11}B$_{carb}$ data is used to reconstruct the variability in surface pH$_{sw}$ on annual timescales for the period 1940 to 2009. These results are then integrated with recent measurements of linear extension, a good indicator of calcification rates, from multiple long *Porites* cores from inner-shelf and mid-shelf reefs in the central GBR (D'Olivo et al., 2013), which includes cores analyzed for boron isotopes reported herein. This enables comparisons to be made between the dynamic environment of inner-shelf reefs, which are subject to terrestrial and anthropogenic influences, and mid-shelf reefs that experience more stable conditions and are less exposed to terrestrial runoff and

pollutants (Lough, 2001; Furnas, 2003; Brodie et al., 2012). Collectively these records of δ^{11}B (this study) and linear extension (D'Olivo et al., 2013) of coral skeletons provide a unique dataset with insight into pH_{sw} variability in a natural coastal system, and how these variations relate to changes in coral calcification and other important environmental parameters (e.g. nutrient flux).

2 Samples and methods

2.1 Instrumental rainfall, river discharge and sea surface temperature records

Monthly rainfall data for Townsville was obtained from the Bureau of Meteorology (http://www.bom.gov.au/climate/data/, 2011). Monthly river discharge and water pH (pH_{rw}) for the Burdekin and Herbert rivers was obtained from the State of Queensland, Department of Environment and Resource Management (DERM; http://watermonitoring.derm.qld.gov.au, 2011). Monthly sea surface temperature (SST) was obtained from the Met Office Hadley Centre's sea ice and sea surface temperature data set, (HadISST1) centred at 18° S and 147° E and with a spatial resolution of 1° × 1° (http://www.metoffice.gov.uk/hadobs/hadisst/, 2014). Inner-shelf average monthly in situ SST for 1993–2008 was obtained from the Australian Institute of Marine Science (AIMS, http://data.aims.gov.au/, 2011). The inner-shelf SST was obtained by averaging temperature logger records at Pandora Reef, Havannah Island, Cleveland Bay, Pioneer Bay, Cattle Bay, and Pelorous Island. Annual data is defined from October to September based on the rainfall seasonal pattern in Queensland, with October marking the start of the warmer summer wet season (Lough, 2007, 2011).

2.2 Water samples

Water samples were collected to characterize the δ^{11}B composition of the plume waters ($\delta^{11}B_{pw}$) in the inner-shelf area during flood events, and to effectively interpret the

Full Screen / Esc

Printer-friendly Version

Interactive Discussion

$\delta^{11}B_{carb}$ coral signal. In February 2007, a total of 29 water samples were collected (by Stephen Lewis, James Cook University) along a northward transect from the mouth of the Burdekin River to Magnetic Island (Fig. 1). In February 2009, a second suite of water samples were collected (by J. P. D'Olivo) from the Burdekin River at the bridge located between the towns of Ayr and Home Hill, as well as seven seawater samples along a northward transect from the mouth of the Burdekin River to Pandora Reef. The presence of discolored water indicated that the river plume had reached all of the sampling sites. After collection, 125 mL of each sample was filtered through a 0.45 μm Teflon membrane and then acidified using 2–3 drops of $\sim 7\,M$ HNO_3. Samples were then stored in acid-cleaned, low-density polyethylene bottles in a cool room. Salinity data was provided by S. Lewis (2009). Water samples were analyzed for B by solution quadrupole ICP-MS using a Varian 820 ICP-MS at the Research School of Earth Sciences at the Australian National University (ANU). ^{10}Be was used as an internal standard spiked at a concentration of 4 ppb. Water samples were diluted according to their salinity by 1000 times with respect to a seawater salinity of 35.

2.3 Sclerochronology and coral sampling for $\delta^{11}B$ analysis

Five cores were drilled from massive *Porites* coral heads from four sites in the central GBR (Fig. 1): Pandora Reef (PAN02) and Havannah Island (HAV06A and HAV09_3) within the inner-shelf, and Rib Reef (RIB09_3) and Reef 17-065 (1709_6) from the mid-outer shelf reefs. All cores exhibit clear and regular annual growth banding. Subsamples representing annual growth increments, from the beginning of each high density band (for mid-shelf corals) or luminescent band (for inner-shelf corals), were milled along the axis of maximum growth of 0.7 cm thick slabs from each core.

2.4 Boron isotope methodology

Boron isotope ratios of all water samples and annual coral subsamples of cores HAV06A, PAN02 and RIB03 were analyzed at the ANU by positive thermal ionization

mass spectrometery (PTIMS) using a Thermo Finnigan TRITON. Annual coral sub-samples of cores HAV09_3 and 1709_6 were analyzed at the University of Western Australia (UWA) by MC-ICPMS using a NU Plasma II. Prior to analysis, samples were cleaned in H_2O_2 (for PTIMS) or in NaOCl (for MC-ICPMS) to remove organic mate-

5 rial, dissolved in HNO_3, and the boron then purified using column chromatography. The boron separation technique used for the PTIMS is based on methodology by Wei et al. (2009) and refined by Trotter et al. (2011). For MC-ICPMS, an ion-exchange resin purification technique was employed using a combination of cation AG 50W-X8 and anion AG 1-X8 resins as described by (McCulloch et al., 2014).

10 All boron isotopic ratios are expressed in the conventional delta notation (δ) relative to the NBS-951 boric acid international standard. Over the course of this study, PTIMS analysis of directly loaded SRM951 standard yielded a mean value of $\delta^{11}B = +0.05$‰ relative to a reference value for this standard of 4.054, with an external precision (2σ) of ± 0.35‰ ($n = 43$) and an internal precision of ± 0.07‰. Repeated analyses of the

15 samples ($n = 46$) gave an average reproducibility of ± 0.2‰ (2σ). A modern coral from Papua New Guinea (NEP B) was used as a secondary working standard. Repeated NEP B analyses gave an average value of 26.35 ± 0.44‰ (2σ, $n = 33$) using PTIMS, and 25.96 ± 0.32‰ (2σ, $n = 70$) using MC-ICPMS. Difference in the $\delta^{11}B_{carb}$ values of coral samples ($n = 8$) analyzed with the PTIMS and MC-ICPMS gave a consistent pos-

20 itive offset of $+0.45$‰. To maintain consistency between the two data sets a $+0.45$‰ correction was applied to the data measured by MC-ICPMS. Measurements of the international carbonate standards Jcp by MC-ICPMS gave a $\delta^{11}B$ value of 24.3 ± 0.34‰ (2σ).

Conversion of $\delta^{11}B_{carb}$ to pH of the calcifying fluid (pH_{cf}) values was determined

25 using the relationship:

$$pH_{cf} = pK_B - \log\left[\frac{\delta^{11}B_{SW} - \delta^{11}B_{carb}}{\alpha_{B3-B4}\delta^{11}B_{carb} - \delta^{11}B_{SW} + 1000(\alpha_{B3-B4} - 1)}\right] \quad (1)$$

Title Page

Abstract | Introduction

Conclusions | References

Tables | Figures

|◄ | ►|

◄ | ►

Back | Close

Full Screen / Esc

Printer-friendly Version

Interactive Discussion

Where $\delta^{11}B_{sw}$ is the B isotope composition of seawater ($\delta^{11}B_{sw} = 39.5\,‰$; Spivack and Edmond, 1986; Foster, 2008) and the B isotope fractionation factor (α_{B3-B4}) of 1.0272 is taken from Klochko et al. (2006). The B dissociation constant (pK_B) was adjusted to the ambient temperature and salinity, the latter especially relevant for corals from the inner-shelf reef region, which is diluted by fresh water during flood events. Seasonal variation in salinity was estimated based on the linear relationship observed between the magnitude of past flood events and corresponding salinity values reported by King et al. (2001) and Walker (1981) near the sampled reefs (Fig. 2).

Average annual salinity values were estimated using the equation given in Fig. 2; considering a mean seawater value of 35.5 and a dilution factor for a period of two months based on the maximum river discharge in each year. Despite limitations with this approach, as flood events are spatially and temporally variable (King et al., 2001; Furnas, 2003), the effect after correcting the pK_B for salinity and temperature on the estimated pH_{sw} value is small ($< {\sim}\,0.01\,pH$ units).

The external pH_{sw} value was estimated following the method and *Porites* sp. specific correction factor of Trotter et al. (2011):

$$pH_{sw} = (pH_{cf} - 5.954)/0.32 \qquad (2)$$

All measured and reconstructed pH_{sw} values are reported relative to the total pH scale.

The $\delta^{11}B$ composition of water samples was analyzed by PTIMS following a simplified purification procedure (cf. coral samples), that omitted the H_2O_2 cleaning step and employed a single AGW50-X8 cation column elution followed by an IRA743 column elution (i.e. the final cation column was omitted). The amount of water sample required to extract and purify 1 µg of B was estimated from the relationship between the measured [B] and salinity (S) in the flood plume ($B = 0.1299(S) + 0.1188$ and $B = 0.1302(S) - 0.0374$; 2007 and 2009, respectively Fig. 3a).

3 Results

3.1 Plume waters boron concentration, δ^{11}B ratios and pH during flood events

Measured [B] and δ^{11}B$_{pw}$ are plotted against salinity of the water samples collected during the flood events of 2007 and 2009 (Fig. 3). Salinity ranges from 0 at the river mouth to 30 at Havannah Island and 26.5 at Pandora Reef. Salinity and [B] concentration during the flood events of 2007 and 2009 show a liner relationship ($r^2 = 0.9834$; $p < 0.0001$; $n = 10$ for 2007 and $r^2 = 0.9915$; $p < 0.0001$; $n = 8$ for 2009), consistent with conservative mixing of boron between seawater and flood-waters.

The flood events sampled in 2007 and 2009 show large differences in the δ^{11}B$_{pw}$ composition of the low salinity flood-waters collected close to the river mouth (Fig. 3). The low δ^{11}B$_{pw}$ (+15‰) measured during the larger 2009 flood event (29 Teraliters) contrasts with the less variable and higher δ^{11}B$_{pw}$ (+42.8‰) of the smaller 2007 flood event (10 Teraliters). River water collected from the Burdekin River Bridge (23 km upstream from the river mouth) during the 2009 flood event had a δ^{11}B$_{pw}$ value of +28‰. Despite the large difference in the δ^{11}B$_{pw}$ values of waters near the river mouth in the two flood events, δ^{11}B$_{pw}$ of samples taken close to the inner-shelf reefs are very similar, with an average δ^{11}B value of 40 ± 0.2‰ (2 S.E.; $n = 2$). This value is identical to seawater samples from Lady Musgrave Island in the southern GBR (δ^{11}B$_{sw} = 39.8 \pm 0.37$‰; 2 S.E.; $n = 2$), and is consistent with previously reported seawater values (Foster et al., 2010). The pH$_{rw}$ of the Burdekin River (Fig. 4; data from the Queensland DERM, 2011) has an average of 7.58 ± 0.46 (2σ), with summer values (7.56 ± 0.41; 2σ) being slightly lower than winter values (7.65 ± 0.35; 2σ).

3.2 Coral δ^{11}B records

3.2.1 Interannual variability

Coral δ^{11}B$_{carb}$ compositions for fives cores give average values that range from 23.6 ± 0.37 to 25.2 ± 0.57‰ over the common period of 1973 to 2002 (Table 2). These values are consistent with previously reported values for *Porites* corals (Hönisch et al., 2004; Pelejero et al., 2005; Wei et al., 2009; Krief et al., 2010). Using Eqs. (1) and (2), these δ^{11}B values translate into reconstructed pH$_{sw}$ values of 7.88 ± 0.07 to 8.19 ± 0.11 (Table 2). The mid-shelf corals have slightly lower δ^{11}B$_{carb}$ (and pH) values than the inner-shelf corals, and are also more variable (±0.37 to ±0.44‰; 2σ) than the inner-shelf corals (±0.5 to ±0.66‰; 2σ). Differences between coral cores are significant (Kruskal–Wallis one way ANOVA on ranks). Pairwise multiple comparison procedures (Tukey Test; $p < 0.05$) indicate that these differences are significant between the three inner-shelf cores and the mid-shelf core 1709_6; mid-shelf core RIB09_3 is only significantly different from inner-shelf core HAV06A. No significant correlation was found between the different δ^{11}B$_{carb}$ coral time series.

Linear regressions applied to the reconstructed annual pH$_{sw}$ time-series for all five coral records show a decrease in time over the full length of each coral record (Fig. 5). This is equivalent to a decrease in pH$_{sw}$ of 0.017 ± 0.008 units per decade for the inner-shelf corals and 0.018 ± 0.007 units per decade for the mid-shelf corals. These rates are consistent with global estimates of 0.017 to 0.019 pH units decrease per decade from 1984 to 2011 based on instrumental data (Dore et al., 2009; Santana-Casiano et al., 2007; Bates et al., 2012), but lower than the 0.041 ± 0.017 pH unit decrease per decade for the period of 1940 to 2004 shown by the δ^{11}B$_{carb}$ coral record from Arlington Reef (mid-reef) in the Central GBR reported previously by Wei et al. (2009). However, the Arlington Reef core exhibited a marked decrease in δ^{11}B$_{carb}$ composition in association with the effects of the severe 1998 bleaching event.

Composite time series for $\delta^{11}B_{carb}$ were obtained for the inner-shelf and mid-shelf corals (Fig. 6) for the periods of 1963 to 2005 and 1973 to 2009 respectively. These are the periods common to more than one core for each region. Composite records were calculated from normalized data by subtracting the mean value and dividing over the standard deviation over the common period of 1966 to 2002. The $\delta^{11}B_{carb}$ annual composite for inner-shelf and mid-shelf records are plotted against time and compared with annual discharge from the Burdekin River, SST, from HadISST1, and coral linear extension rates from D'Olivo et al. (2013). The composite $\delta^{11}B_{carb}$ time series for inner-shelf corals shows significant correlation with river discharge, SST, and coral extension rates (Table 3). The mid-shelf record shows a weaker but still significant correlation with SST.

The 8 year low pass filter applied to the composite reconstructed pH_{sw} data derived from the three inner-shelf $\delta^{11}B_{carb}$ coral records (Fig. 7) reveals semi-decadal variation which is not observed in the mid-shelf $\delta^{11}B_{carb}$ data. Similar variability is observed in inner-shelf coral extension rates and calcification when periods of slower growth coincide with higher terrestrial runoff (D'Olivo et al., 2013). It follows that enhanced $\delta^{11}B_{carb}$ (higher pH) signals coincide with periods of increased river discharge and slower extension rates.

4 Discussion

4.1 Variations in river and seawater $\delta^{11}B$ during flood events

Mean pH_{rw} values for the period 1995 to 2006 of 7.6 ± 0.4 (2σ) for the Burdekin River (Fig. 4) and 7.1 ± 0.4 (2σ) for the Herbert River (data from the Queensland DERM, 2011) indicate that low pH fresh water, in comparison to pH_{sw}, is introduced into the coastal area of the GBR during wet periods. The pH_{rw} data for the Burdekin River shows significant sub-annual variability, with a decrease in pH during some high discharge events, but there is no consistent seasonal pattern. This indicates that factors

other than the amount of discharge or rainfall determine the pH_{rw}, and may reflect variability that is related to the nature of the material being carried by the river, rather than the rainfall.

Boron isotope compositions of flood water sampled near the mouth of the Burdekin River were higher during the larger flood event of 2009 ($\delta^{11}B_{pw}$ = +42.8 ‰) than during the smaller flood event of 2007 ($\delta^{11}B_{pw}$ = +15 ‰). This contrasts with data reported by Barth (1998) from the Elbe Estuary in Germany, where water samples collected near the river mouth during a minor flood event had a significantly lower $\delta^{11}B$ value than samples collected during a major flood event. In the case of the Elbe Estuary, the heavier $\delta^{11}B$ composition measured during an extreme flood event was explained by the admixture of a ^{11}B-rich component mainly from rainwater (Barth, 1998). The $\delta^{11}B_{pw}$ from different flood events can vary significantly, as shown by the 2007 and 2009 events. Given that the $\delta^{11}B_{rw}$ is likely influenced by various factors, including both the type and amount of terrigenous material carried by the river during flood events, as well as the source of the river runoff and nature of the catchment, more work is needed to characterize B dynamics and isotope fractionation mechanisms during flood events. Although the $\delta^{11}B_{pw}$ values during 2007 and 2009 show a large variation close to the Burdekin River mouth, the $\delta^{11}B_{pw}$ values near the inner-shelf reefs are typical of ocean waters (i.e. $\delta^{11}B \sim 40$ ‰).

4.2 Origin of interannual $\delta^{11}B_{carb}$ variability in corals

The results shown in Fig. 5 and corresponding correlations suggest a relationship between coral $\delta^{11}B_{carb}$ and both ambient seawater temperature and terrestrial runoff, particularly for the inner-shelf region of the GBR. However the interannual pH_{sw} variability of ±0.01 pH units, which is directly attributable to temperature and salinity changes due to river run-off (Fig. 8c), contrasts with the interannual variability of more than ±0.07 pH units reconstructed from the $\delta^{11}B_{carb}$ compositions for the inner-shelf and mid-shelf

corals. Possible explanations for the interannual variability observed in $\delta^{11}B_{carb}$ (reconstructed pH_{sw}) are examined below.

4.2.1 Clay adsorption and sediments

A possible explanation for interannual $\delta^{11}B_{carb}$ variations for inner-shelf corals comes from the adsorption of B onto sediments and clays that are delivered to the inner shelf region by rivers. Clays preferentially remove the lighter isotope ^{10}B from seawater (Palmer et al., 1987; Barth, 1998). This results in the respective depletion of ^{11}B in marine clays but enrichment in seawater, and is the accepted explanation for the heavy isotopic composition of seawater (e.g. 39.61 ± 0.04 ‰; Foster et al., 2010) relative to average continental crust (Spivack and Edmond, 1986; Palmer et al., 1987; Barth, 1998). Given the large silt and clay wash load transported from the Burdekin River (Belperio, 1979), fractionation of $\delta^{11}B$ between the dissolved and adsorbed B phases could have a significant effect on the $\delta^{11}B$ of seawater. However, the conservative mixing of B along the salinity transect (Fig. 3) indicates that boron is not being quantitatively removed from the plume waters by clays, and that the clay material is already in equilibrium with the river water before entering the ocean. Similar results have been reported by Barth (1998) and Xiao et al. (2007). Furthermore, the oceanic $\delta^{11}B_{pw}$ values near the reefs during flood events and the low B concentration of river waters require that, at the reef sites, the $\delta^{11}B$ signal is dominated by seawater. Finally, large $\delta^{11}B_{carb}$ interannual variations occur on the mid-shelf reefs where there is no clay-dominated terrestrial runoff.

4.2.2 Effect of nutrient enrichment and biological productivity on pH_{sw}

River discharge is an important source of particulate and dissolved nutrients as well as sediments to the inner-shelf area of the GBR (King et al., 2002; Devlin and Brodie, 2005), with about 90 % of the particulate and dissolved nutrients introduced during flood events (Mitchell and Bramley, 1997; Furnas, 2003). Most particulate matter and

sediments are deposited within a few kilometers (~ 10 km) of river mouths, at a salinity value of < 10 (Wolanski and Jones, 1981), whereas dissolved nutrients are carried greater distances, up to about 200 km along the coast (Devlin and Brodie, 2005). Once the turbidity decreases and low light levels are no longer limiting, dissolved nutrients are rapidly taken up by primary producers resulting in phytoplankton blooms (Furnas, 2003; Devlin and Brodie, 2005; Brodie et al., 2010a). These blooms do not usually develop until the salinity reaches ~ 25, typically between 50 and 200 km from the river mouth (Devlin and Brodie, 2005) which correspond to the position of the inner-shelf coral reefs that are the subject of this study.

Considering NO_3^- as the main form of nitrogen sourced from the Burdekin River into the inner-shelf area of the GBR (Furnas, 2003), plankton productivity will result in the decrease of seawater CO_2, increase in alkalinity, and uptake of H^+ (Gattuso et al., 1999). A strong coupling between CO_2 dynamics and large phytoplankton bloom events has been observed at Kane'ohe Bay, Hawaii, sufficiently such that the reef system changes from being a source of CO_2 to a CO_2 sink (Drupp et al., 2011). At Kane'ohe Bay, bloom events are fueled by nutrient inputs following rainfall and terrestrial runoff events. The enhanced productivity is reflected by increased phytoplankton biomass from ~ 2 to $\sim 6\,\mu g\,L^{-1}$ chl a, which draws down pCO_2 by ~ 100 ppm (Drupp et al., 2011). Similar large changes in phytoplankton biomass occur in the central GBR, where chl a increases from between 0.3 and $0.7\,\mu g\,L^{-1}$ chl a (Brodie et al., 2007) and up to 1 to $20\,\mu g\,L^{-1}$ chl a within flood plumes (Devlin and Brodie, 2005; Brodie et al., 2010b). When the decrease in pCO_2 of 100 ppm reported by (Drupp et al., 2011) is included into the modeled response shown in Fig. 8, an increase of 0.2 pH units is observed during flood events. It follows that the higher $\delta^{11}B_{carb}$ (and reconstructed pH_{sw}) values from the inner shelf reefs during periods of high river discharge are consistent with decreased pCO_2 and increased pH_{sw} due to the stimulation of phytoplankton production.

4.2.3 Cross-shelf differences in coral $\delta^{11}B_{carb}$ and reconstructed pH_{sw}

A systematic cross-shelf pattern is observed in $\delta^{11}B_{carb}$ (and reconstructed pH_{sw}) with both average values and interannual variability being greater for inner-shelf corals compared to mid-shelf corals (Table 2). This cross-shelf pattern is consistent with the available, yet limited, pH_{sw} data that comprises summer (2007) values of 8.14 ± 0.003 Gagliano et al. (2010) measured at Magnetic Island in the inner-shelf area, and summer 2012 values of 8.03 ± 0.03 measured at Davies Reef Albright et al. (2013).

It is not surprising to find differences in reconstructed pH_{sw} values between reefs as the GBR is characterized by significant spatial gradients in seawater parameters (e.g. temperature and water quality), especially across different shelfal environments (D'Olivo et al., 2013; Cantin and Lough, 2014; Fabricius et al., 2014). These spatial differences could account, for example, for the lower interannual variation of the coral $\delta^{11}B_{carb}$ records from the mid-shelf reefs compared to inner-shelf reefs, through the decreased influence of river runoff on mid-shelf reefs as previously suggested by Wei et al. (2009).

The reason for the lack of correlation between the $\delta^{11}B_{carb}$ records at nearby reefs, specifically Pandora and Havannah Island, is unclear. Differences in biological driven effects (e.g. species or gender related) or local variability to environmental parameters (e.g. light regime) are possible explanations. Nevertheless, the overall good agreement between the composite $\delta^{11}B_{carb}$ coral record and the terrestrial runoff indices is encouraging, suggesting that multi-core replication (Lough, 2004; Jones et al., 2009) and consideration of ambient environmental conditions are essential when interpreting $\delta^{11}B_{carb}$ records. Further analyses of additional records from the same area should help clarify the uncertainties and improve our understanding of the $\delta^{11}B_{carb}$ seawater proxy in dynamic reefal systems that characterise inshore environments. A multi-proxy approach should also prove helpful to confirm the results from this study, but also to determine the response of corals to specific environmental parameters.

4.2.4 Relationship between $\delta^{11}B_{carb}$ (reconstructed pH$_{sw}$) and coral growth rates

Calcification and linear extension rates of inner-shelf corals show a long-term decrease from the period of 1930 to 2008 (Lough, 2008; D'Olivo et al., 2013). This decrease

[5] has been attributed to factors ranging from thermal stress, bleaching, eutrophication, and ocean acidification (Cooper et al., 2008; Lough, 2008; De'ath et al., 2009; D'Olivo et al., 2013). The present study reveals that decadal-scale wet periods with increased terrestrial runoff in the central GBR coincide with periods of reduced inner-shelf coral growth (Fig. 7). This is despite $\delta^{11}B_{carb}$ evidence for concurrent higher reconstructed

[10] pH$_{sw}$ and hence higher seawater carbonate saturation state. Given the apparently more favorable seawater carbonate chemistry (high pH$_{sw}$ and Ω_{arag}) for coral growth during wet periods, other factors such as degraded water quality must clearly be responsible for the decline in extension rates observed during wet periods. Direct monitoring of seawater carbonate system parameters would greatly help understand the response

[15] of the complex inner-shelf systems to changes in water quality.

4.2.5 Physiological controls on coral calcification

The coral pH$_{cf}$ values calculated from the measured $\delta^{11}B_{carb}$ compositions (Table 2) indicate that corals elevate the pH at the site of calcification, in agreement with previous studies (Al-Horani et al., 2003; Venn et al., 2011; McCulloch et al., 2012). This

[20] elevation of pH$_{cf}$ for massive *Porites* grown in the natural environment is estimated to be 0.41 ± 0.022 for the inner-shelf corals and 0.43 ± 0.027 for the mid-shelf corals. The latter values were estimated using the coral pH$_{cf}$ values in Table 2 and the directly measured pH$_{sw}$ summer value of 8.14 from Gagliano et al. (2010) as an independent reference value for the inner-shelf region, and an average pH$_{sw}$ annual value of 8.06

[25] from Albright et al. (2013) for the mid-shelf region.

Aside from pH up-regulation at the calcification site (McCulloch et al., 2012), other processes involved in promoting aragonite precipitation include the transport of ions to

the mineralization site and the synthesis of an organic matrix (Allemand et al., 2004; Venn et al., 2011). Inhibition or reduced activity of these processes has been associated with significant reduction of calcification in other studies (Tambutte et al., 1996; Allemand et al., 1998, 2004; Al-Horani et al., 2003). The reduction in growth of inner-shelf coral may thus be explained by the effects of river discharge that could include increased shading, turbidity, sedimentation, or competition for carbon from the photosynthetic activity of zooxanthellae. These factors can affect enzyme activity or synthesis of the organic matrix involved in the calcification process (Tambutte et al., 1996; Allemand et al., 1998, 2004; Al-Horani et al., 2003) because energy and DIC required by these processes is reallocated into cleaning or mucus production (Riegl and Branch, 1995; Telesnicki and Goldberg, 1995; Philipp and Fabricius, 2003). Therefore, it should not be surprising to find reduced growth during wet periods and hence degraded water quality despite conditions of higher pH and Ω_{arag}. Critically, this suggests the still over-riding importance of local reef water quality relative to the still subordinate longer-term effects of ocean acidification.

In contrast to the inner-shelf reefs, the $\delta^{11}B_{carb}$ record of the mid-shelf corals shows no significant relationship to river discharge, consistent with the reduced effects of river flood plumes. Extreme flood events can however occasionally reach the mid-shelf reefs, especially when offshore winds occur (King et al., 2002). This is confirmed by the presence of more subdued luminescent bands in coral records from Rib Reef that coincide with some large river discharge events. Nevertheless, coral linear extension and calcification at both mid-shelf and outer-shelf reef locations shows an increase over the last ∼ 50 years, coincident with the rise in temperature over this period (D'Olivo et al., 2013). This observed increase in coral calcification, despite the decrease in the reconstructed pH_{sw}, indicates that ocean acidification has so far played a secondary role in impacting coral calcification in the mid-shelf region.

5 Summary and conclusions

Coral $\delta^{11}B_{carb}$ values show cross-shelf variability with higher average and amplitude values characteristic of the corals closer to the coast. The reconstructed pH_{sw} values calculated from the coral $\delta^{11}B_{carb}$ indicate that, in their natural environment, massive *Porites* up-regulate pH_{cf} by ~ 0.4 units. Variability in coral $\delta^{11}B_{carb}$ show an interannual range in reconstructed pH_{sw} from ~ 0.07 pH units in mid-shelf corals to ~ 0.11 pH units in inner-shelf corals, compared to a much smaller long term (1940 to 2009) trend of ~ 0.017 pH unit decrease per decade. This rate of change is consistent with previous estimates of decreasing surface pH_{sw} from $p CO_2$ driven ocean acidification. Results from $\delta^{11}B_{carb}$ and coral growth indicate that terrestrial runoff has a significant effect on inner-shelf reef environments. We propose that phytoplankton blooms, fueled by increased nutrient inputs from river plume waters, drive the drawdown of dissolved CO_2, and thus increase the pH in surface seawaters. Consequently on a local-scale, the inner-shelf reefs of the GBR exhibit high rates of nutrient driven production, and following river discharge events, temporarily counter the effects of ocean acidification. However, despite the higher pH_{sw} and Ω_{sw} we observe an associated decrease in coral linear extension and calcification (D'Olivo et al., 2013), which is contrary to expectations where coral calcification increases with increasing Ω_{sw} (McCulloch et al., 2012). This suggests that the effects of large flood events on water quality (e.g. increased shading, turbidity, sedimentation, or competition for carbon by up-regulated photosynthetic activity of zooxanthellae) are the dominant cause of reduced coral growth. This study demonstrates the value of coral $\delta^{11}B$ as a paleo-proxy for reconstructing past pH_{sw} changes, as well as the importance of disentangling the effects of local water quality, which is not only relevant for the inner-shelf region of the GBR but other coral systems worldwide.

The Supplement related to this article is available online at doi:10.5194/bgd-11-11443-2014-supplement.

References

Al-Horani, F. A., Al-Moghrabi, S. M., and de Beer, D.: The mechanism of calcification and its relation to photosynthesis and respiration in the scleractinian coral *Galaxea fascicularis*, Mar. Biol., 142, 419–426, doi:10.1007/s00227-002-0981-8, 2003.

Albright, R., Langdon, C., and Anthony, K. R. N.: Dynamics of seawater carbonate chemistry, production, and calcification of a coral reef flat, central Great Barrier Reef, Biogeosciences, 10, 6747–6758, doi:10.5194/bg-10-6747-2013, 2013.

Allemand, D., Tambutt, E. E., Girard, J. P., and Jaubert, J.: Organic matrix synthesis in the scleractinian coral *Stylophora pistillata*: role in biomineralization and potential target of the organotin tributyltin, J. Exp. Biol., 201, 2001–2009, 1998.

Allemand, D., Ferrier-Pages, C., Furla, P., Houlbreque, F., Puverel, S., Reynaud, S., Tambutte, E., Tambutte, S., and Zoccola, D.: Biomineralisation in reef-building corals: from molecular mechanisms to environmental control, C. R. Palevol., 3, 453–467, doi:10.1016/j.crpv.2004.07.011, 2004.

Andersson, A. J., Mackenzie, F. T., and Lerman, A.: Coastal ocean and carbonate systems in the high CO_2 world of the anthropocene, Am. J. Sci., 305, 875–918, 2005.

Barth, S.: $^{11}B/^{10}B$ variations of dissolved boron in a freshwater-seawater mixing plume (Elbe Esturary, North Sea), Mar. Chem., 62, 1–14, 1998.

Bates, N. R., Amat, A., and Andersson, A. J.: Feedbacks and responses of coral calcification on the Bermuda reef system to seasonal changes in biological processes and ocean acidification, Biogeosciences, 7, 2509–2530, doi:10.5194/bg-7-2509-2010, 2010.

Bates, N. R., Best, M. H. P., Neely, K., Garley, R., Dickson, A. G., and Johnson, R. J.: Detecting anthropogenic carbon dioxide uptake and ocean acidification in the North Atlantic Ocean, Biogeosciences, 9, 2509–2522, doi:10.5194/bg-9-2509-2012, 2012.

Belperio, A.: The combined use of wash loads and bed material load rating curves for the calculation of total load: an example from the Burdekin River, Australia, Catena, 6, 317–329, 1979.

Brodie, J., Fabricius, K., De'ath, G., and Okaji, K.: Are increased nutrient inputs responsible for more outbreaks of crown-of-thorns starfish? An appraisal of the evidence, Mar. Pollut. Bull., 51, 266–278, doi:10.1016/j.marpolbul.2004.10.035, 2005.

Brodie, J., De'ath, G., Devlin, M., Furnas, M., and Wright, M.: Spatial and temporal patterns of near-surface chlorophyll a in the Great Barrier Reef lagoon, Mar. Freshwater. Res., 58, 342–353, 2007.

Brodie, J., Devlin, M., Haynes, D., and Waterhouse, J.: Assessment of the eutrophication status of the Great Barrier Reef lagoon (Australia), Biogeochemistry, 106, 281–302, doi:10.1007/s10533-010-9542-2, 2010a.

Brodie, J., Schroeder, T., Rohde, K., Faithful, J., Masters, B., Dekker, A., Brando, V., and Maughan, M.: Dispersal of suspended sediments and nutrients in the Great Barrier Reef lagoon during river-discharge events: conclusions from satellite remote sensing and concurrent flood-plume sampling, Mar. Freshwater. Res., 61, 651–664, 2010b.

Brodie, J., Wolanski, E., Lewis, S., and Bainbridge, Z.: An assessment of residence times of land-sourced contaminants in the Great Barrier Reef lagoon and the implications for management and reef recovery, Mar. Pollut. Bull., 65, 267–279, doi:10.1016/j.marpolbul.2011.12.011, 2012.

Cantin, N. E. and Lough, J. M.: Surviving Coral Bleaching Events: Porites Growth Anomalies on the Great Barrier Reef, PLoS ONE, 9, e88720, doi:10.1371/journal.pone.0088720, 2014.

Cooper, T. F., De'ath, G., Fabricius, K. E., and Lough, J. M.: Declining coral calcification in massive *Porites* in two nearshore regions of the northern Great Barrier Reef, Glob. Change Biol., 14, 529–538, doi:10.1111/j.1365-2486.2007.01520.x, 2008.

D'Olivo, J. P., McCulloch, M. T., and Judd, K.: Long-term records of coral calcification across the central Great Barrier Reef: assessing the impacts of river runoff and climate change, Coral Reefs, 32, 999–1012, doi:10.1007/s00338-013-1071-8, 2013.

De'ath, G. and Fabricius, K.: Water quality as a regional driver of coral biodiversity and macroalgae on the Great Barrier Reef, Ecol. Appl., 20, 840–850, 2010.

Coral records of reef-water pH across the central Great Barrier Reef, Australia

J. P. D'Olivo et al.

Title Page

Abstract   Introduction

Conclusions   References

Tables   Figures

◀◀   ▶▶

◀   ▶

Back   Close

Full Screen / Esc

Printer-friendly Version

Interactive Discussion

De'ath, G., Lough, J. M., and Fabricius, K. E.: Declining coral calcification on the Great Barrier Reef, Science, 323, 116–119, doi:10.1126/science.1165283, 2009.

Devlin, M. J. and Brodie, J.: Terrestrial discharge into the Great Barrier Reef Lagoon: nutrient behavior in coastal waters, Mar. Pollut. Bull., 51, 9–22, doi:10.1016/j.marpolbul.2004.10.037, 2005.

Dickson, A. G.: Thermodynamics of the dissociation of boric acid in synthetic seawater from 273.15 to 318.15 K, Deep-Sea Res., 37, 755–766, 1990.

Dickson, A. G. and Millero, F. J.: A comparison of the equilibrium-constants for the dissociation of carbonic-acid in seawater media, Deep-Sea Res., 34, 1733–1743, 1987.

Doney, S. C., Fabry, V. J., Feely, R. A., and Kleypas, J. A.: Ocean acidification: the other CO_2 problem, Annu. Rev. Mar. Sci., 1, 169–192, doi:10.1146/annurev.marine.010908.163834, 2009.

Dore, J. E., Lukas, R., Sadler, D. W., Church, M. J., and Karl, D. M.: Physical and biogeochemical modulation of ocean acidification in the central North Pacific, P. Natl. Acad. Sci. USA, 106, 12235–12240, doi:10.1073/pnas.0906044106, 2009.

Drupp, P., De Carlo, E. H., Mackenzie, F. T., Bienfang, P., and Sabine, C. L.: Nutrient inputs, phytoplankton response, and CO_2 variations in a semi-enclosed subtropical embayment, Kaneohe Bay, Hawaii, Aquat. Geochem., 17, 473–498, doi:10.1007/s10498-010-9115-y, 2011.

Duarte, C. M., Hendriks, I. E., Moore, T. S., Olsen, Y. S., Steckbauer, A., Ramajo, L., Carstensen, J., Trotter, J. A., and McCulloch, M.: Is ocean acidification an open-ocean syndrome? Understanding anthropogenic impacts on seawater pH, Estuar. Coast., 36, 221–236, doi:10.1007/s12237-013-9594-3, 2013.

Fabricius, K. E., Logan, M., Weeks, S., and Brodie, J.: The effects of river run-off on water clarity across the central Great Barrier Reef, Mar. Pollut. Bull., 84, 191–200, doi:10.1016/j.marpolbul.2014.05.012, 2014.

Falter, J. L., Lowe, R. J., Zhang, Z., and McCulloch, M.: Physical and biological controls on the carbonate chemistry of coral reef waters: effects of metabolism, wave forcing, sea level, and geomorphology, PloS ONE, 8, e53303, doi:10.1371/journal.pone.0053303, 2013.

Foster, G. L.: Seawater pH, $p$$CO_2$ and [CO_{2-3}] variations in the Caribbean Sea over the last 130 kyr: a boron isotope and B/Ca study of planktic foraminifera, Earth Planet. Sc. Lett., 271, 254–266, doi:10.1016/j.epsl.2008.04.015, 2008.

Title Page

Abstract | Introduction

Conclusions | References

Tables | Figures

◄ | ►►

◄ | ►

Back | Close

Full Screen / Esc

Printer-friendly Version

Interactive Discussion

Foster, G. L., Pogge von Strandmann, P. A. E., and Rae, J. W. B.: Boron and magnesium isotopic composition of seawater, Geochem. Geophy. Geosy., 11, Q08015, doi:10.1029/2010gc003201, 2010.

Frithsen, J. B., Keller, A. A., and Pilson, M. E. Q.: Effects of Inorganic Nutrient Additions in Coastal Areas: a Mesocosm Experiment; Data Report, Marine Ecosystems Research Laboratory, Graduate School of Oceanography, University of Rhode Island, 1985.

Furnas, M.: Catchments and Corals: Terrestrial Runoff to the Great Barrier Reef, Australian Institute of Marine Science and Reef CRC, Townsville, Australia, 2003.

Gagliano, M., McCormick, M. I., Moore, J. A., and Depczynski, M.: The basics of acidification: baseline variability of pH on Australian coral reefs, Mar. Biol., 157, 1849–1856, doi:10.1007/s00227-010-1456-y, 2010.

Gattuso, J.-P., Frankignoulle, M., and Smith, S. V.: Measurement of community metabolism and significance in the coral reef CO_2 source-sink debate, P. Natl. Acad. Sci. USA, 96, 13017–13022, 1999.

Hemming, N. G. and Hanson, G. N.: Boron isotopic composition and concentration in modern marine carbonates, Geochim. Cosmochim. Ac., 56, 537–543, 1992.

Hinga, K. R.: Effects of pH on coastal marine phytoplankton, Mar. Ecol.-Prog. Ser., 238, 281–300, 2002.

Hönisch, B., Hemming, N. G., Grottoli, A. G., Amat, A., Hanson, G. N., and Buma, J.: Assessing scleractinian corals as recorders for paleo-pH: empirical calibration and vital effects, Geochim. Cosmochim. Ac., 68, 3675–3685, doi:10.1016/j.gca.2004.03.002, 2004.

Jones, P. D., Briffa, K. R., Osborn, T., Lough, J., van Ommen, T. D., Vinther, B. M., Luterbacher, J., Wahl, E. R., Zwiers, F. W., Mann, M. E., Schmidt, G. A., Ammnn, C. M., Buckley, B. M., Cobb, K. M., Esper, J., Goosse, H., Graham, N., Jansen, E., Kiefer, T., Kull, C., Küttel, E., Mosley-Thompson, E., Overpeck, J. T., Riedwyl, N., Schultz, M., Tudhope, A. W., Villalba, R., Wanner, H., Wolff, E., and Xoplaki, E.: High-resolution palaeoclimatology of the last millennium: a review of current status and future prospects, Holocene, 19, 3–49, 2009.

King, B., McAllister, F., Wolanski, E., Done, T., and Spagnol, S.: River plume dynamics in the central Great Barrier Reef, in: Oceanographic Processes of Coral Reefs: Physical and Biological Links in the Great Barrier Reef, edited by: Wolanski, E., CRC Press, Boca Raton, 145–160, 2001.

King, B., McAllister, F., and Done, T.: Modelling the impact of the Burdekin, Herbert, Tully and Johnstone River plumes on the Central Great Barrier Reef, CRC Reef Research Centre, Townsville, 44, 2002.

Kleypas, J. A.: Geochemical consequences of increased atmospheric carbon dioxide on coral reefs, Science, 284, 118–120, doi:10.1126/science.284.5411.118, 1999.

Klochko, K., Kaufman, A. J., Yao, W., Byrne, R. H., and Tossell, J. A.: Experimental measurement of boron isotope fractionation in seawater, Earth Planet. Sc. Lett., 248, 276–285, doi:10.1016/j.epsl.2006.05.034, 2006.

Krief, S., Hendy, E. J., Fine, M., Yam, R., Meibom, A., Foster, G. L., and Shemesh, A.: Physiological and isotopic responses of scleractinian corals to ocean acidification, Geochim. Cosmochim. Ac., 74, 4988–5001, doi:10.1016/j.gca.2010.05.023, 2010.

Lewis, S. E., Shields, G. A., Kamber, B. S., and Lough, J. M.: A multi-trace element coral record of land-use changes in the Burdekin River catchment, NE Australia, Palaeogeogr. Palaeocl., 246, 471–487, doi:10.1016/j.palaeo.2006.10.021, 2007.

Liu, Y., Liu, W., Peng, Z., Xiao, Y., Wei, G., Sun, W., He, J., Liu, G., and Chou, C.-L.: Instability of seawater pH in the South China Sea during the mid-late Holocene: evidence from boron isotopic composition of corals, Geochim. Cosmochim. Ac., 73, 1264–1272, doi:10.1016/j.gca.2008.11.034, 2009.

Lough, J. M.: Climate variability and change on the Great Barrier Reef, in: Oceanographic Processes of Coral Reefs: Physical and Biological Links in the Great Barrier Reef, edited by: Wolanski, E., CRC Press, Boca Raton, Florida, 269–300, 2001.

Lough, J. M.: A strategy to improve the contribution of coral data to high-resolution paleoclimatology, Palaeogeogr. Palaeocl., 204, 115–143, doi:10.1016/s0031-0182(03)00727-2, 2004.

Lough, J. M.: Tropical river flow and rainfall reconstructions from coral luminescence: Great Barrier Reef, Australia, Paleoceanography, 22, PA2218, doi:10.1029/2006pa001377, 2007.

Lough, J. M.: Coral calcification from skeletal records revisited, Mar. Ecol.-Prog. Ser., 373, 257–264, doi:10.3354/meps07398, 2008.

Lough, J. M.: Measured coral luminescence as a freshwater proxy: comparison with visual indices and a potential age artefact, Coral Reefs, 30, 169–182, doi:10.1007/s00338-010-0688-0, 2011.

McCulloch, M. T., Falter, J., Trotter, J., and Montagna, P.: Coral resilience to ocean acidification and global warming through pH up-regulation, Nat. Clim. Change, 2, 623–627, doi:10.1038/nclimate1473, 2012.

McCulloch, M. T., Fallon, S., Wyndham, T., Hendy, E., Lough, J. M., and Barnes, D. J.: Coral record of increased sediment flux to the inner Great Barrier Reef since European settlement, Nature, 421, 727–730, doi:10.1038/Nature01361, 2003.

McCulloch, M. T., Holcomb, M., Rankenburg, K., and Trotter, J.: Rapid, high-precision measurements of boron isotopic compositions in marine carbonates, Rapid Commun. Mass Sp., submitted, 2014.

Merhbach, C., Culberson, C. H., Hawley, J. E., and Pytkowicz, R. M.: Measurement of the apparent dissociation constants of carbonic acid in seawater at atmospheric pressure, Limnol. Oceanogr., 18, 897–907, 1973.

Mitchell, A. W. and Bramley, R. G. V.: Export of Nutrients and Suspended Sediment from the Herbert River Catchment During a Flood Event Associated with Cyclone Sadie, Cyclone Sadie Flood Plumes in the GBR Lagoon: Composition and Consequences, Workshop series, No. 22. 1997, Great Barrier Reef Marine Park Authority, 1997.

Palmer, M. R., Spivack, A. J., and Edmond, J. M.: Temperature and pH controls over isotopic fractionation during adsorption of boron on marine clay, Geochim. Cosmochim. Ac., 51, 2139–2323, 1987.

Pelejero, C., Calvo, E., McCulloch, M. T., Marshall, J. F., Gagan, M. K., Lough, J. M., and Opdyke, B. N.: Preindustrial to modern interdecadal variability in coral reef pH, Science, 309, 2204–2207, doi:10.1126/science.1113692, 2005.

Philipp, E. and Fabricius, K.: Photophysiological stress in scleractinian corals in response to short-term sedimentation, J. Exp Mar. Biol. Ecol., 287, 57–78, 2003.

Reynaud, S., Hemming, N. G., Juillet-Leclerc, A., and Gattuso, J. P.: Effect of pCO$_2$ and temperature on the boron isotopic composition of the zooxanthellate coral Acropora sp, Coral Reefs, 23, 539–546, doi:10.1007/s00338-004-0399-5, 2004.

Riegl, B. and Branch, G. M.: Effects of sediment on the energy budgets of four scleractinian (Bourne 1900) and five alcyonacean (Lamouroux 1816) corals, J. Exp Mar. Biol. Ecol., 186, 259–275, 1995.

Salisbury, J., Green, M., Hunt, C., and Campbell, J.: Coastal acidification by rivers: a threat to shellfish?, EOS T. Am. Geophys. Un., 89, 513–528, 2008.

Santana-Casiano, J. M., González-Dávila, M., Rueda, M.-J., Llinás, O., and González-Dávila, E.-F.: The interannual variability of oceanic CO$_2$ parameters in the northeast Atlantic subtropical gyre at the ESTOC site, Global Biogeochem. Cy., 21, GB1015, doi:10.1029/2006gb002788, 2007.

Shinjo, R., Asami, R., Huang, K.-F., You, C.-F., and Iryu, Y.: Ocean acidification trend in the tropical North Pacific since the mid-20th century reconstructed from a coral archive, Mar. Geol., 342, 58–64, doi:10.1016/j.margeo.2013.06.002, 2013.

Simpson, J. J. and Zirino, A.: Biological-control of pH in the Peruvian coastal upwelling area, Deep-Sea Res., 27, 733–744, 1980.

Spivack, A. J. and Edmond, J. M.: Determination of boron isotope ratios by thermal ionization mass-spectrometry of the dicesium metaborate cation, Anal. Chem., 58, 31–35, 1986.

Suzuki, A., Kawahata, H., Ayukai, T., and Goto, K.: The oceanic CO_2 system and carbon budget in the Great Barrier Reef, Australia, Geophys. Res. Lett., 28, 1243–1246, 2001.

Sweatman, H., Delean, S., and Syms, C.: Assessing loss of coral cover on Australia's Great Barrier Reef over two decades, with implications for longer-term trends, Coral Reefs, 30, 521–531, doi:10.1007/s00338-010-0715-1, 2011.

Tambutte, E., Allemand, D., Mueller, E., and Jaubert, J.: A compartmental appproach to the mechanism of calcification in hermatypic corals, J. Exp. Biol., 199, 1029–1041, 1996.

Telesnicki, G. J. and Goldberg, W. M.: Effects of turbidity on the photosynthesis and respiration of two south Florida Reef coral species, B. Mar. Sci., 57, 527–539, 1995.

Trotter, J., Montagna, P., McCulloch, M., Silenzi, S., Reynaud, S., Mortimer, G., Martin, S., Ferrier-Pagès, C., Gattuso, J.-P., and Rodolfo-Metalpa, R.: Quantifying the pH "vital effect" in the temperate zooxanthellate coral *Cladocora caespitosa*: validation of the boron seawater pH proxy, Earth Planet. Sc. Lett., 303, 163–173, doi:10.1016/j.epsl.2011.01.030, 2011.

Vengosh, A., Kolodny, Y., Starinsky, A., Chivas, A. R., and Mcculloch, M. T.: Coprecipitation and isotopic fractionation of boron in modern biogenic carbonates, Geochim. Cosmochim. Ac., 55, 2901–2910, 1991.

Venn, A., Tambutte, E., Holcomb, M., Allemand, D., and Tambutte, S.: Live tissue imaging shows reef corals elevate pH under their calcifying tissue relative to seawater, PloS ONE, 6, e20013, doi:10.1371/journal.pone.0020013, 2011.

Walker, T.: Seasonal salinity variations in Cleveland Bay, Northern Queensland, Aust. J Mar. Fresh. Res., 32, 143–149, 1981.

Wei, G., McCulloch, M. T., Mortimer, G., Deng, W., and Xie, L.: Evidence for ocean acidification in the Great Barrier Reef of Australia, Geochim. Cosmochim. Ac., 73, 2332–2346, doi:10.1016/j.gca.2009.02.009, 2009.

Wolanski, E. and Jones, M.: Physical properties of the Great Barrier Reef lagoon waters near Townsville. I. Effects of Burdekin River floods, Aust. J Mar. Fresh. Res., 32, 305–319, 1981.

Title Page

Abstract | Introduction

Conclusions | References

Tables | Figures

◄ | ►

◄ | ►

Back | Close

Full Screen / Esc

Printer-friendly Version

Interactive Discussion

Xiao, Y., Liao, B., Wang, Z., Wei, H., and Zhao, Z.: Isotopic composition of dissolved boron and its geochemical behavior in a freshwater-seawater mixture at the estuary of the Changjiang (Yangtze) River, Chinese J. Geochem., 26, 105–113, 2007.

Coral records of reef-water pH across the central Great Barrier Reef, Australia

J. P. D'Olivo et al.

Back · Close

Full Screen / Esc

Printer-friendly Version

Interactive Discussion

Table 1. Periods covered by coral core samples analysed.

Region	Reef	Core id	Period covered
Inner-shelf	Havannah Is.	HAV06A	1966–2005
		HAV09_3	1940–2009
	Pandora	PAN02	1963–2002
Mid-shelf	Rib	RIB09_3	1964–2009
	17-065	1709_6	1973–2009

Table 2. Mean annual values (2σ) for coral $\delta^{11}B_{carb}$, pH_{cf}, and pH_{sw}. The reconstructed pH_{sw} values were estimated using Eq. (2) to correct for the pH offset at the site of calcification. Average values are calculated over the common period of 1973–2002. The slope is the annual rate of change for the reconstructed pH_{sw} time series derived by linear regression of the full length of each core (see Table 1).

	Core	$\delta^{11}B_{carb}$ Average	pH_{cf} Average	pH_{sw} Average	Slope (pH unit yr^{-1})
Inner-shelf	HAV06A	25.17 ± 0.57	8.58 ± 0.04	8.19 ± 0.11	−0.0020 ± 0.003
	HAV09_3	24.15 ± 0.5	8.54 ± 0.03	8.08 ± 0.1	−0.0023 ± 0.0011
	PAN02	24.54 ± 0.66	8.54 ± 0.04	8.07 ± 0.13	−0.0008 ± 0.0038
Mid-shelf	RIB09_3	24.2 ± 0.44	8.51 ± 0.03	8 ± 0.09	−0.0023 ± 0.002
	1709_6	23.6 ± 0.37	8.48 ± 0.02	7.88 ± 0.07	−0.0013 ± 0.0021

Table 3. Pearson correlation coefficients (r) and corresponding p values for correlations of annual composite coral $\delta^{11}B_{carb}$ time series from the inner-shelf (1964 to 2005) and mid-shelf (1973 to 2009) with Burdekin River runoff, SST from HadISST1 and coral linear extension rates for the corresponding region taken from D'Olivo et al. (2013).

	River runoff (log ML)		SST (°C)		Lin ext (cm yr^{-1})	
	r	p value	r	p value	r	p value
$\delta^{11}B_{carb}$ inner-shelf ($n = 42$)	0.565	0.0001	−0.387	0.0103	−0.418	0.0053
$\delta^{11}B_{carb}$ mid-shelf ($n = 37$)	0.147	0.386	−0.42	0.0096	−0.302	0.0733
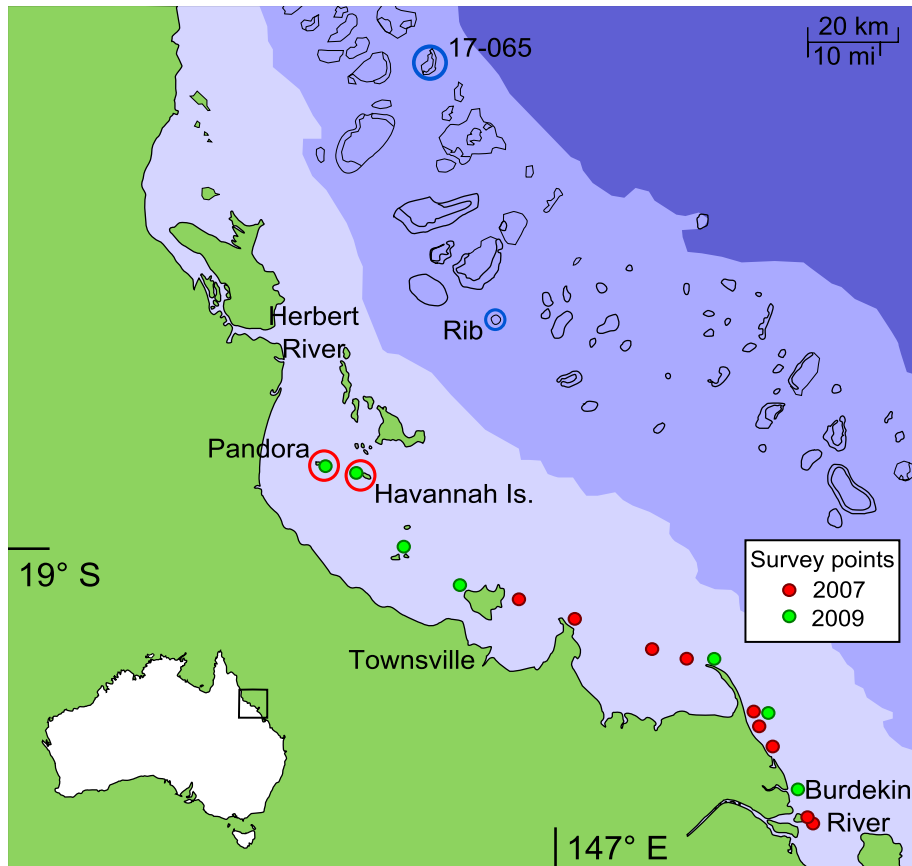
Figure 1. Map of the central area of the GBR showing locations water sample and coral core collection sites: Pandora Reef and Havannah Island in the inner-shelf; Rib Reef and 17-065 Reef in the mid-shelf region; water sample collection sites during the flood events of 2007 and 2009.
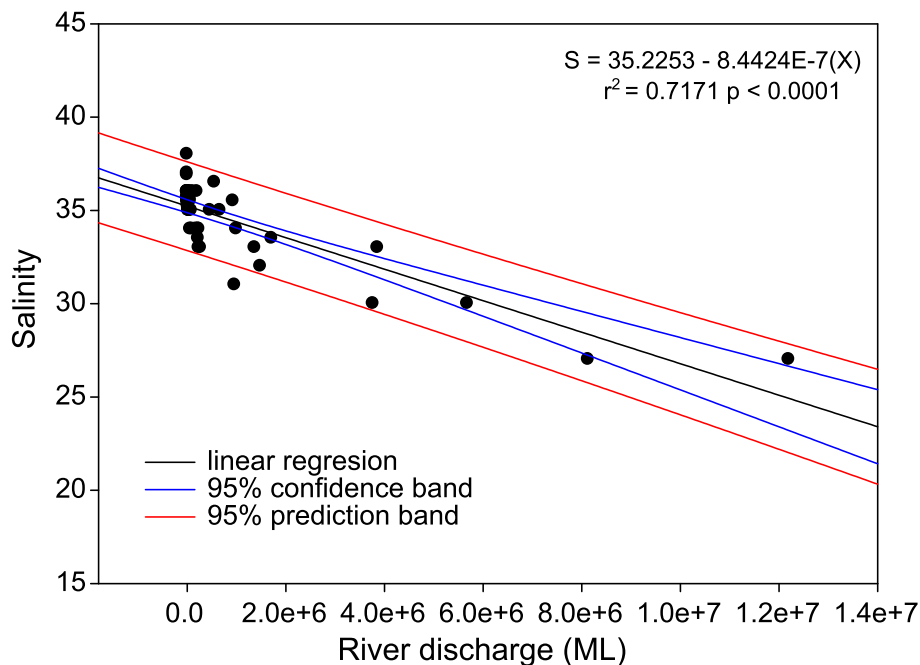
Figure 2. Comparison of minimum salinity values from the central inner-shelf region near Pandora Reef and Havannah Island King et al. (2001) and Cleveland Bay Walker (1981) with discharge runoff from the Burdekin River. The regression line and corresponding equation were used to estimate the dilution of seawater at the inner-shelf reefs from river discharge. The confidence bands indicate the uncertainty associated to the regression lines, while the prediction bands relate to the distribution of values within 95 % probability.

Title Page

Abstract | Introduction

Conclusions | References

Tables | Figures

|◄ | ►|

◄ | ►

Back | Close

Full Screen / Esc

Printer-friendly Version

Interactive Discussion
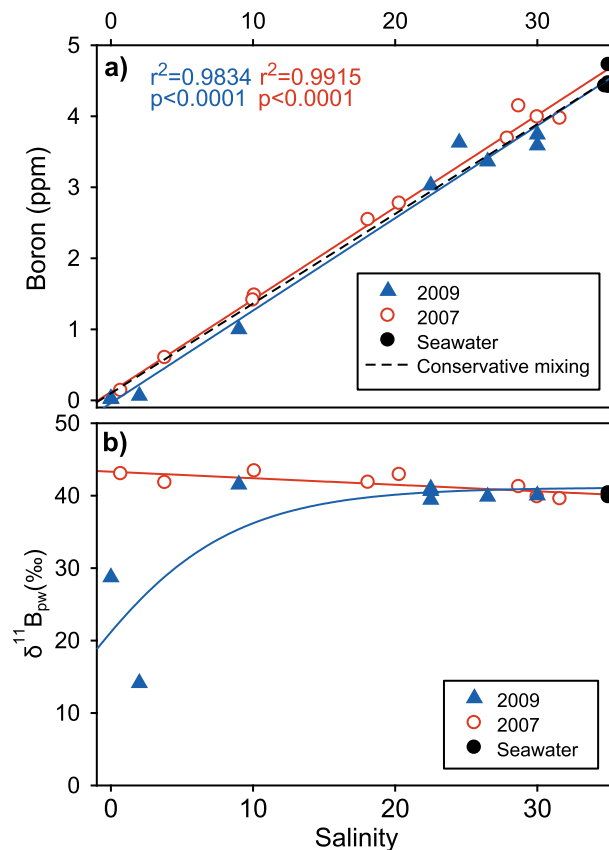
Figure 3. (a) Boron concentration plotted against salinity of waters from the flood events of 2007 and 2009. A linear regression through the data is compared to the theoretical conservative mixing relationship based on a seawater end-member with 4.52 mg B L^{-1} at $S = 35$. **(b)** Boron isotope composition of waters along salinity transects from the 2007 and 2009 flood events.

11474
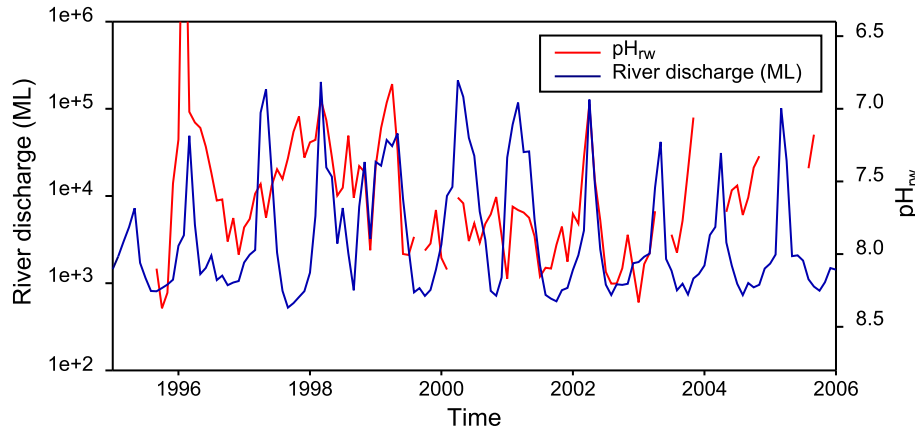
Full Screen / Esc

Figure 4. Monthly discharge and pH_{rw} of the Burdekin River (data obtained from Queensland DERM, 2011; pH scale not available).
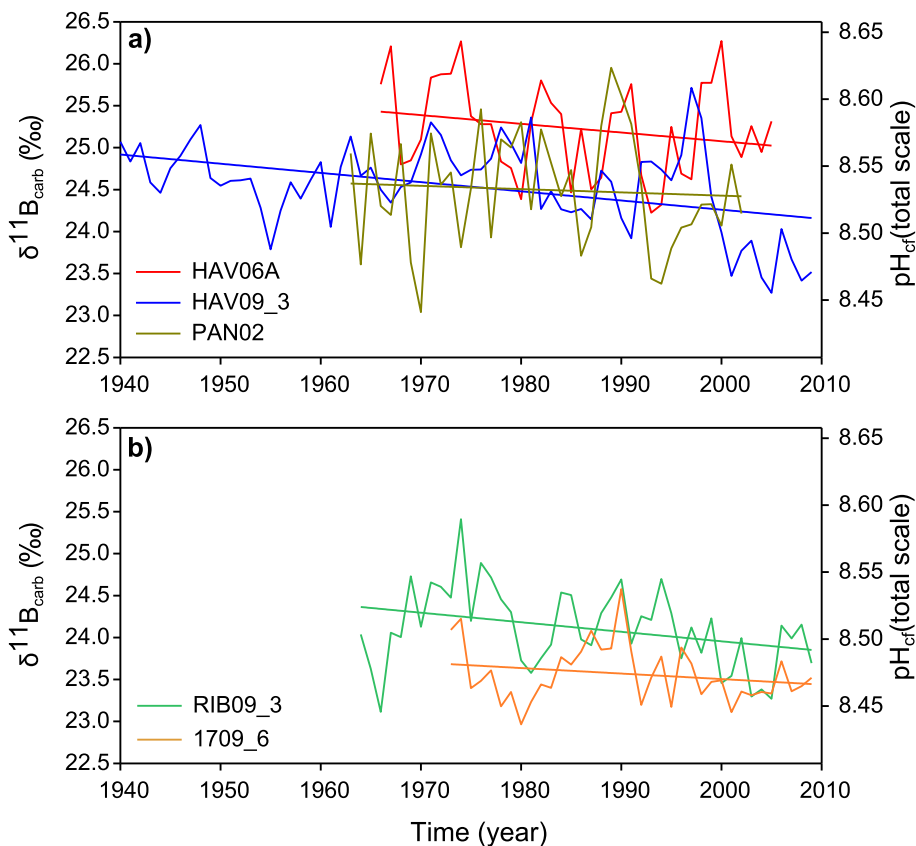
Figure 5. Annual time-series and linear regressions for $\delta^{11}B_{carb}$ and corresponding pH_{cf} from the compositions of coral samples from: **(a)** the inner-shelf reefs of Havannah Island and Pandora Reef, and **(b)** the mid-shelf reefs of Rib Reef and 17-065.
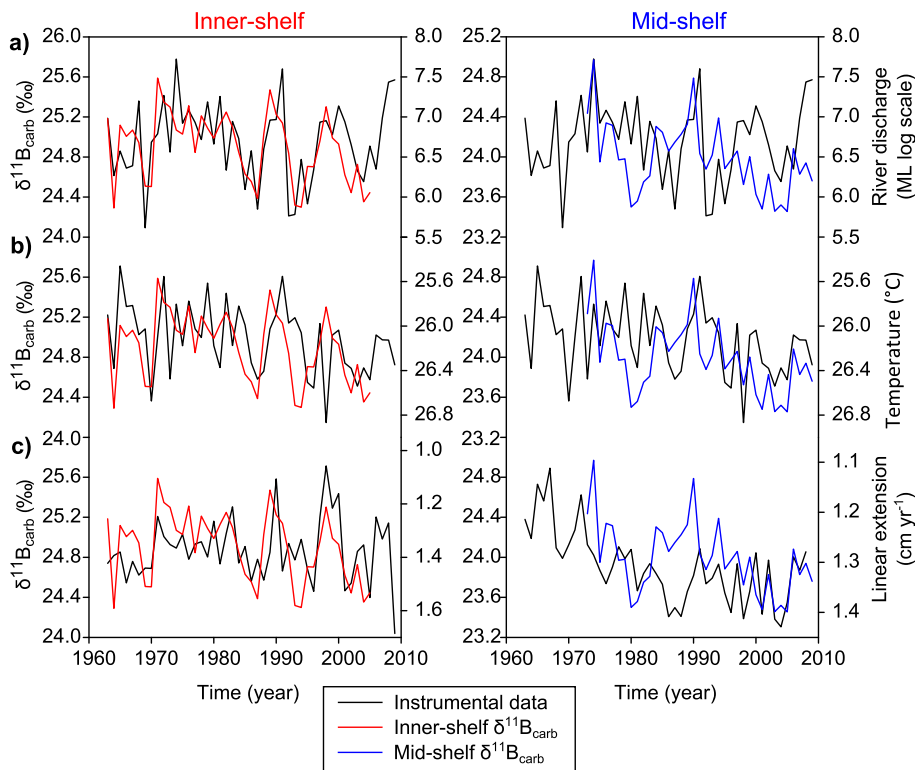
Figure 6. Annual composite $\delta^{11}B_{carb}$ time series for the inner-shelf corals and mid-shelf corals compared to annual discharge from the Burdekin River **(a)**, SST from HadISST1 **(b)**, and coral linear extension rates from D'Olivo et al. (2013) for the corresponding inner-shelf or mid-shelf regions **(c)**. Note that the temperature and linear extension axis has been reversed to facilitate comparisons.
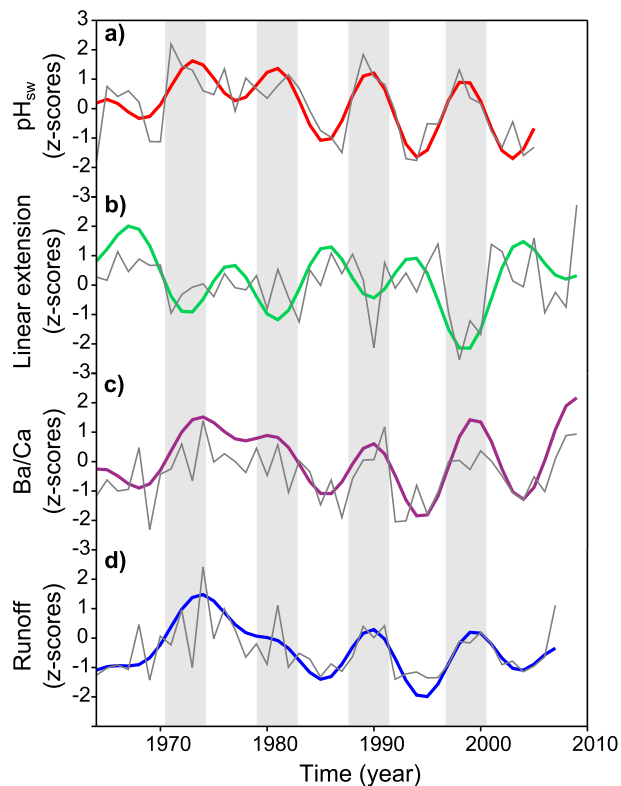
Figure 7. Normalized annual (grey) and smoothed (coloured 8 year low band pass filter) time-series for: **(a)** the inner-shelf composite reconstructed pH_{sw} obtained from $\delta^{11}B_{carb}$ coral records, **(b)** averaged linear extension of inner-shelf in the central GBR (D'Olivo et al., 2013), terrestrial influx indicated by **(c)** discharge from the Burdekin River and **(d)** coral Ba/Ca data from Pandora and Havannah Is (McCulloch et al., 2003).
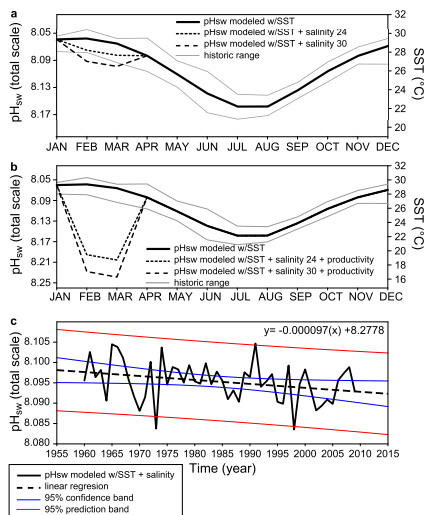
Figure 8. (a) Estimated seasonal pH_{sw} changes based on in situ SST (AIMS; 2011) variation. The grey lines define the range of historic maximum and minimum values for any given month. Changes in pH_{sw} resulting from a hypothetical two month decrease in salinity to values of 30 and 24 due to river discharge are shown. **(b)** Estimated seasonal pH_{sw} changes as in **(a)** including a pCO_2 drawdown of 100 ppm during flood events due to phytoplankton production based on results from Drupp et al. (2011). **(c)** Estimated annual pH_{sw} changes based on reconstructed SST (HadISST1) and salinity changes associated with flood events obtained from the equation in Fig. 2. The confidence bands represent the uncertainty associated with the regression fit, whereas the prediction bands indicate the distribution of values within 95 % probability. pH_{sw} values were estimated considering a seawater end-member with a TA of 2260 mmol kgsw^{-1} and DIC of 1920 mmol kgsw^{-1} measured by Suzuki et al. (2001), salinity, and a river water end-member with a of TA 787.7 mmol kgsw^{-1} and DIC of 811.1 mmol kgsw^{-1} estimated from TA and pH_{rw} data obtained from DERM. Calculations were made using CO_2 SYS with carbonate constants K1 and K2 from Merhbach et al. (1973) refit by Dickson and Millero (1987) and for sulfate from Dickson (1990) with atmospheric pressure = 1 atm.